III International Conference on Particle-based Methods – Fundamentals and Applications
PARTICLES 2013
M. Bischoff, E. Oñate, D.R.J. Owen, E. Ramm & P. Wriggers (Eds)

DISCRETE ELEMENT MODEL FOR BRITTLE MATERIALS

G. KOVAL[1], B.D. LE[2] AND C. CHAZALLON[3]

National Institute of Applied Sciences of Strasbourg
24 Boulevard de la Victoire - 67000 Strasbourg - France
[1] georg.koval@insa-strasbourg.fr

[2] badanh.le@insa-strasbourg.fr

[3] cyrille.chazallon@insa-strasbourg.fr

Key words: rupture, discrete element method, brittle materials

Abstract. We adopt the discrete element method (DEM) to study the fracture behavior of brittle materials. We propose an approach which relates crack initiation to crack growth. The material consists of a set of particles in contact, which allows us to derive an expression for the stress intensity factor as a function of the contact forces and displacements. A classical failure criterion, based on the material's toughness, is then adopted for the analysis of crack propagation, represented by the loss of cohesion forces between particles. Afterwards, we apply our discrete criterion to uncracked materials under homogenous stress conditions, obtaining a Rankine like behavior. The work results in a simple discrete model which is totally compatible to continuum mechanics, where no calibration tests are required, in contrast to most of discrete approaches.

1 INTRODUCTION

The linear elastic fracture mechanics remains one of the most used approaches to model crack propagation in a structure. Many numerical schemes were derived from continuum mechanics to analyse material rupture like finite differences, finite element method (FEM), integral quations, extended finite element method (XFEM), etc. The most popular are FEM based schemes, adopted in many different conditions (static, dynamical, thermal, etc.). However some difficulties like the mesh refinement at the crack tip (and during its progression) do exist. The XFEM schemes simplify the refinement problem with enrichment functions describing the crack behavior, though convergence problems may appear. Another important intrinsic issue, associated to continuous approaches is the integration of macroscopic failure criteria (i.e. for uncracked structures) with classical fracture mechanics.

In order to minimize these disadvantages, we propose to apply the discrete element method (DEM) [2, 4] to study the rupture of brittle materials. The description of the

material as a group of particles in contact makes the propagation of cracks technically easy and intuitive. The efforts are transmitted by forces, while the material properties are described at the (microscopic) contact level. Macroscopic behavior like elasticity, plasticity, viscosity, etc. are strictly related to contact constitutive laws.

The main goal of our work is to propose a discrete approach where macroscopic rupture is naturally related to crack propagation (fracture mechanics). At the same time, we intend to avoid calibration procedures keeping the model totally compatible to continuous approaches. We begin with a description of the contact behavior in elasticity on section 2, followed by the resulting material behavior on section 3. On section 4, we discuss the description of the stresses and strains on the discrete approach, which is fundamental for the crack propagation analysis in mixed mode, presented on section 5. We examine an extension of the discret rupture criterion for uncracked materials under homogeneous stresses on section 6. Finally, we present the conclusions of the work.

2 CONTACT MODEL

The basic interaction between two particles can be described by the simple model shown in Figure 1. We may define $\underline{n}^{ij}$, the normal vecteur, oriented from the center of a particule i to the center of a particule j, and $\underline{t}^{ij}$, the tangential vecteur, orthogonal to $\underline{n}^{ij}$ and positively oriented. The contact force between particles i and j has a normal and a tangential component (Figure 2), respectively $\underline{N}^{ij} = \underline{N}_e^{ij} + \underline{N}_v^{ij}$ and $\underline{T}^{ij} = \underline{T}_e^{ij} + \underline{T}_v^{ij}$, both depending on two contributions.

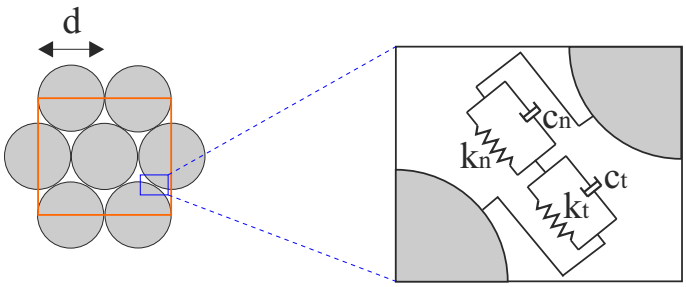

Figure 1: Contact model.

The elastic term of the normal force, $\underline{N}_e^{ij} = k_n \delta_n^{ij} \underline{n}^{ij}$, is a function of the normal displacement δ_n^{ij} and of the normal stiffness k_n. Similarly, the elastic term of the tangential force, $\underline{T}_e^{ij} = k_t \delta_t^{ij} \underline{t}^{ij}$, is a function of the tangential displacement δ_t^{ij} and of the tangential stiffness k_t.

The inelastic term of the normal force $\underline{N}_v^{ij} = c_n \dot{\delta}_n^{ij} \underline{n}^{ij}$ depend on a normal viscous damping parameter c_n and on the time derivative of the normal displacement $\dot{\delta}_n^{ij}$. In the same way, the inelastic term of the tangential force $\underline{T}_v^{ij} = c_t \dot{\delta}_t^{ij} \underline{t}^{ij}$ is based on a tangential viscous damping parameter c_t and on the time derivative of the tangential displacement

$\dot{\delta}_t^{ij}$. The viscous parameters c_n and c_t are defined as small fractions of $\sqrt{mk_n}$ (where m is the particle mass) and induce negligible inelastic effects.

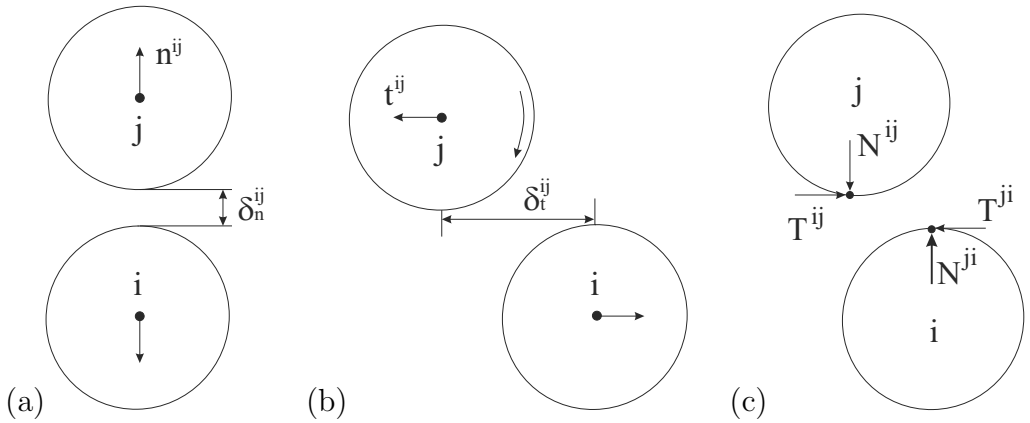

Figure 2: (a) Normal displacement, (b) tangential displacement and (c) associated contact forces between two particles.

3 PARTICLE STRUCTURE AND ELASTIC BEHAVIOR

We adopt a $2D$ close-packing distribution of particles, as shown on Figure 3a, to represent a linear elastic isotropic material (Figure 3b). On a discret approach, the relation between relative position of the particles and contact forces is analogous to strain and stress relation in a continuous approach. It can be shown [6, 8] that normal and tangential stiffness k_n and k_t are directly related to Young's modulus E and Poisson's ratio ν. In plane stress, for a close-packing structure, we have:

$$\begin{aligned} k_n &= \tfrac{1}{\sqrt{3}(1-\nu)} E, \\ k_t &= \tfrac{1-3\nu}{1+\nu} k_n = \tfrac{1-3\nu}{\sqrt{3}(1-\nu^2)} E. \end{aligned} \tag{1}$$

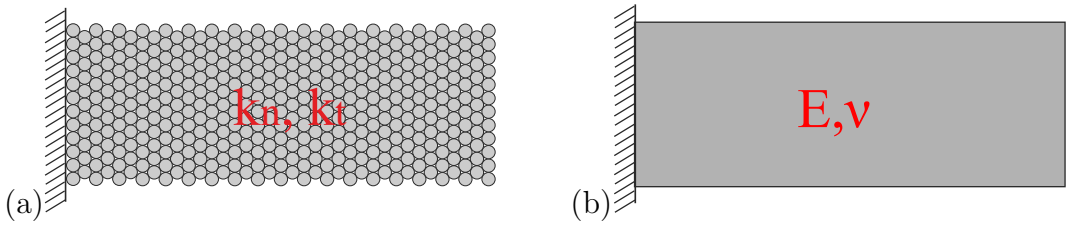

Figure 3: (a) Periodic structure of the discrete material and (b) its continuous equivalence.

4 MEAN STRESSES AND STRAINS ON THE DISCRETE MEDIUM

We determine mean values of the components of the tensors of stress and strain based on the behavior of one pair of contacts associated to three particles (i, j and k) in contact: ki and kj (Figure 4a), near a crack under a given loading (Figure 4b). We define a local coordinate system (n, t), where t virtually connect both contacts and for which n is an orthogonal axis.

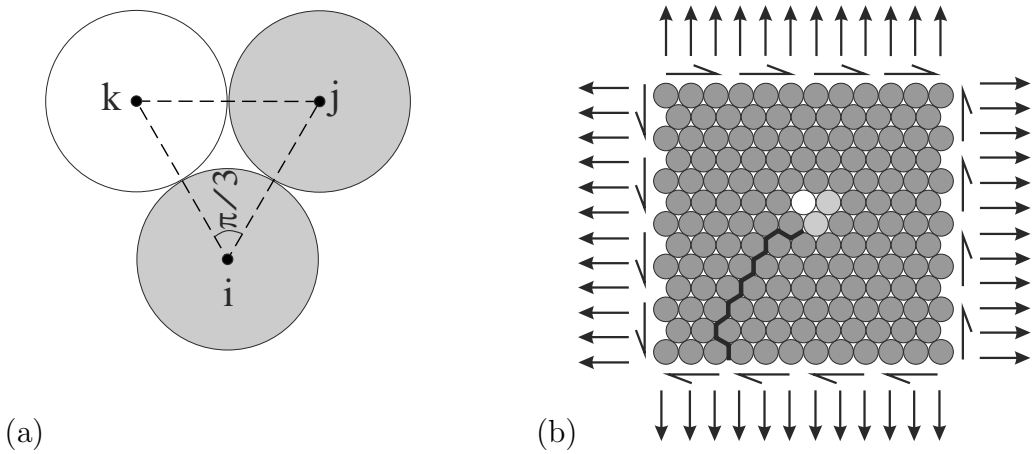

Figure 4: (a) Adjacent contacts at the (b) crack tip in a discrete medium.

The components of the resultant contact force in (n, t) coordinate system (respectively f_n and f_t, see Figure 5) can be written:

$$\begin{aligned} f_n &= \left(N^{ki}\sqrt{3} + T^{ki} + N^{kj}\sqrt{3} - T^{kj}\right)/2, \\ f_t &= \left(-N^{ki} + T^{ki}\sqrt{3} + N^{kj} + T^{kj}\sqrt{3}\right)/2. \end{aligned} \tag{2}$$

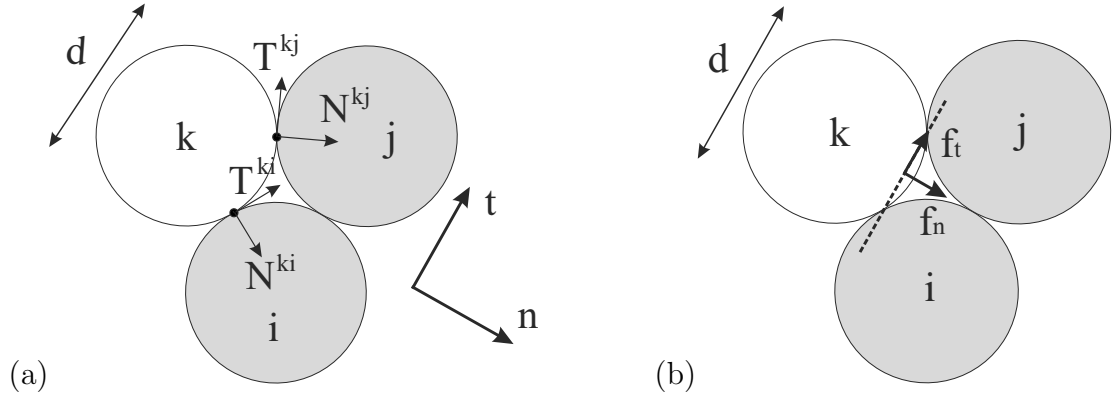

Figure 5: (a) Contact forces and (b) their resultants for an adjacent pair of contacts.

We can associate mean stresses to these forces, considering a length of a particle diameter d:

$$\begin{aligned} \overline{\sigma}_n &= f_n/d, \\ \overline{\sigma}_t &= f_t/d. \end{aligned} \tag{3}$$

The contacts ki and kj may present normal and tangential displacements (respectively δ_n^{ki} and δ_t^{ki}, δ_n^{kj} and δ_t^{kj}). Mean strain values (Figure 6a) can be derived from these contact displacements, considering the dimensions of the particle structure (Figure 6b):

$$\begin{aligned} \overline{\varepsilon}_{nn} &= \left(\delta_n^{ki}\sqrt{3} + \delta_n^{kj}\sqrt{3} + \delta_t^{ki} - \delta_t^{kj}\right)/(2d\sqrt{3}), \\ \overline{\varepsilon}_{tt} &= \left(\delta_n^{ki} + \delta_n^{kj} - \delta_t^{ki}\sqrt{3} + \delta_t^{kj}\sqrt{3}\right)/(4d). \end{aligned} \tag{4}$$

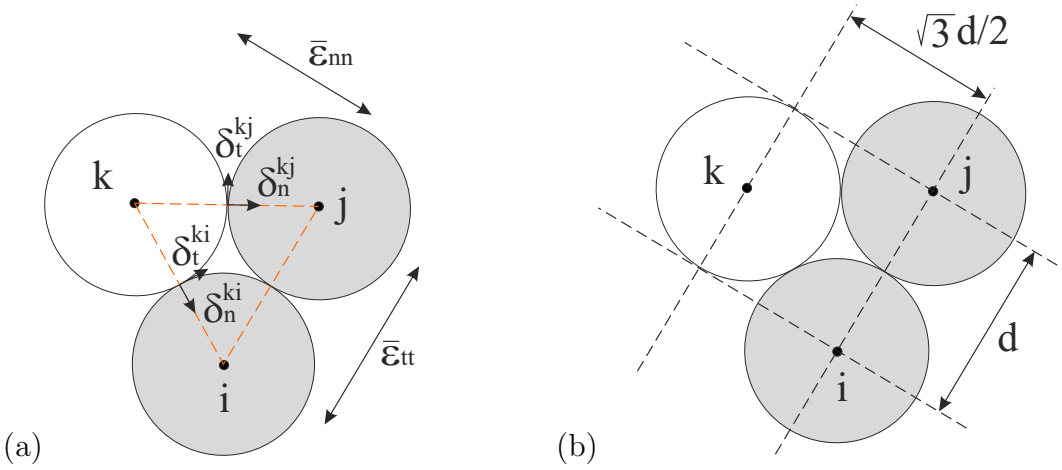

Figure 6: (a) Contact displacements, mean strains and (b) associated dimensions of the particle structure.

4.1 Principal stresses and strains

The complete stress tensor (in $2D$) can be expressed by the principal stresses $\overline{\sigma}_I$ and $\overline{\sigma}_{II}$ and their orientation. Let us call β the angle between (n, t) and the coordinate system associated to the principal stresses. This principle can be extended to the mean stress values on the discret medium (Figure 7a). After a force balance (Figure 7b), the principal stresses may be calculated as:

$$\begin{aligned} \overline{\sigma}_I &= \overline{\sigma}_n + \overline{\sigma}_t \tan(\beta), \\ \overline{\sigma}_{II} &= \overline{\sigma}_n - \overline{\sigma}_t / \tan(\beta). \end{aligned} \tag{5}$$

For an isotropic elastic material, principal stresses are directly related to principal strains ($\overline{\varepsilon}_I$ and $\overline{\varepsilon}_{II}$) by the expression:

$$\begin{bmatrix} \overline{\varepsilon}_I & 0 \\ 0 & \overline{\varepsilon}_{II} \end{bmatrix} = \frac{1+\nu}{E} \begin{bmatrix} \overline{\sigma}_I & 0 \\ 0 & \overline{\sigma}_{II} \end{bmatrix} - \frac{\nu}{E}(\overline{\sigma}_I + \overline{\sigma}_{II}) \begin{bmatrix} 1 & 0 \\ 0 & 1 \end{bmatrix}. \tag{6}$$

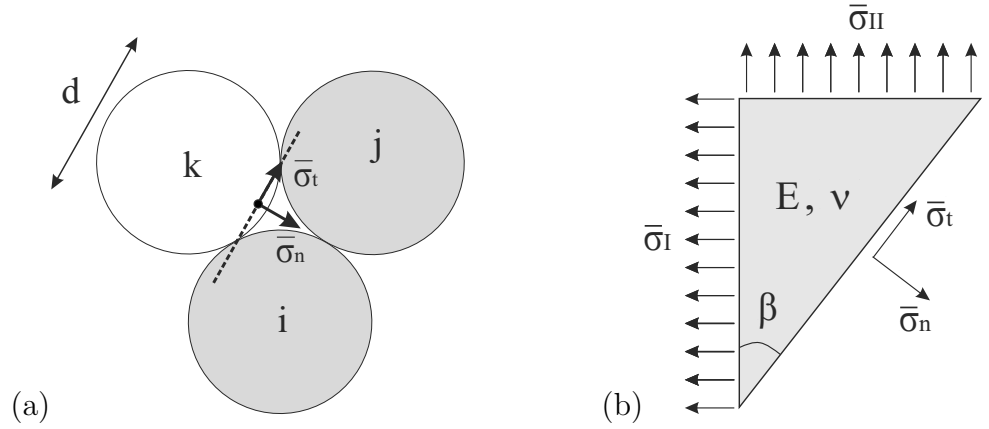

Figure 7: (a) Mean stresses $\overline{\sigma}_n$ and $\overline{\sigma}_t$, and (b) their relation to the stress field of an equivalent continuous medium.

Stress and strain tensors have the same orientation defined by β. It means that mean strain values $\overline{\varepsilon}_{nn}$ and $\overline{\varepsilon}_{tt}$ are equal to

$$\begin{aligned} \overline{\varepsilon}_{nn} &= \overline{\varepsilon}_I \cos^2\beta + \overline{\varepsilon}_{II} \sin^2\beta, \\ \overline{\varepsilon}_{tt} &= \overline{\varepsilon}_I \sin^2\beta + \overline{\varepsilon}_{II} \cos^2\beta. \end{aligned} \tag{7}$$

After some algebraic work on Equations 5, 6 and 7, β can be simply expressed by quantities related to the force and displacement on the discret medium ($\overline{\sigma}_n$, $\overline{\sigma}_t$, $\overline{\varepsilon}_{nn}$ and $\overline{\varepsilon}_{tt}$):

$$\beta = -\frac{1}{2} \arctan\left(\frac{2\overline{\sigma}_t}{\frac{E}{1-\nu}(\overline{\varepsilon}_{nn} + \overline{\varepsilon}_{tt}) - 2\overline{\sigma}_n} \right). \tag{8}$$

Thus the values of the principal stresses are easily evaluated by Equation 5.

5 CRACK PROPAGATION IN MIXED MODE

The stress field near a plane crack can be described based on a polar coordinate system with its origin conveniently placed at the crack tip (Figure 8). For an isotropic elastic material, we may write [5]:

$$\sigma_{\theta\theta}(r,\theta) = \frac{K_{\theta\theta}(\theta)}{\sqrt{2\pi r}},$$
$$\sigma_{r\theta}(r,\theta) = \frac{K_{r\theta}(\theta)}{\sqrt{2\pi r}}, \tag{9}$$
$$\sigma_{rr}(r,\theta) = \frac{K_{rr}(\theta)}{\sqrt{2\pi r}},$$

where $K_{\theta\theta}$, $K_{r\theta}$ and K_{rr} are the effective stress intensity factors and θ is the relative angle defined by the tangent direction at the crack tip.

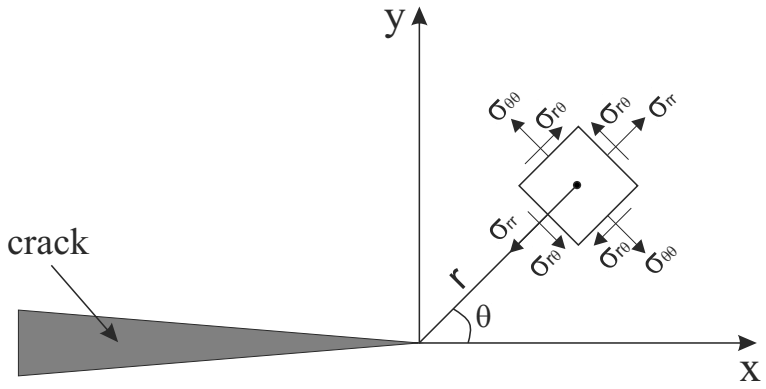

Figure 8: Stresses near a crack tip.

The maximum circunferential tensile stress [3], states that a crack may potentially propagate following a direction θ_0 which maximizes the circumferential stress $\sigma_{\theta\theta}(r,\theta)$ (and minimizes the tangential stress $\sigma_{r\theta}(r,\theta) = 0$). The crack is stable if $K_{\theta\theta}(\theta_0)$ remains lower than the material toughness K_{IC} and propagates if $K_{\theta\theta}$ reaches K_{IC} [5].

5.1 Determination of the effective stress intensity factor $K_{\theta\theta}$

The stress intensity factor $K_{\theta\theta}$ must be obtained for a certain direction θ_0, orthogonal to the direction of the principal stress. The maximum circumferential tensile stress $\overline{\sigma}_{\theta\theta}(\theta_0)$ is then defined as (see Figure 7a):

$$\overline{\sigma}_{\theta\theta}(\theta_0) = \overline{\sigma}_I, \ if \ \beta \leq \pi/4,$$
$$\overline{\sigma}_{\theta\theta}(\theta_0) = \overline{\sigma}_{II}, \ if \ \beta > \pi/4. \tag{10}$$

The mean value of $\sigma_{\theta\theta}(r,\theta_0)$ (Equation 9), is obtained by integration over $0 \leq r \leq d$. The equality of this result to Equation 10 allows us to determine $K_{\theta\theta}(\theta_0)$:

$$K_{\theta\theta}(\theta_0) = \overline{\sigma}_{\theta\theta}(\theta_0)\sqrt{\frac{\pi d}{2}}. \tag{11}$$

In practice, we calculate the stress intensity factor $K_{\theta\theta}(\theta_0)$ for each pair of neighbor contacts. The analysis of all contact pairs eliminates any difficulty of finding crack tips. When $K_{\theta\theta}(\theta_0)$ reaches the value of the material toughness K_{IC}, the cohesion forces of the most tensioned contact of the pair are set to zero, giving rise to the propagation of the crack at the proximity of this contact.

5.2 Numerical results of pre-cracked samples

Numerical test of pre-cracked samples allow us to verify the convergence of the formulation for fracture analysis by the comparaison to theoretical results.

We adopt a system of units defined by some fundamental parameters. The diameter d and the mass m of the particles are the units of length and mass, respectively. To simplify, we suppose that the $2D$ systems present a thickness equal to d. We take K_{IC} as toughness unit, consequently we get $T = \sqrt{m/(K_{IC}\sqrt{d})}$ as time unit, and $K_{IC}/\sqrt{d}$ as stress unit. For the normal stiffness, we choose $k_n = 10^4 K_{IC}/\sqrt{d}$, consistent with the small strain hypothesis. The ratio between tangential and normal stiffness $k_t/k_n = 0.2$ implies in a Poisson's ratio $\nu = 0.25$ (without any considerable effect in plane fracture problems). Finally, a small value of viscous damping $c_n = c_t = 0.65\sqrt{mK_{IC}\sqrt{d}}$ is adopted in all simulations.

The samples (with simple and double cracks) are subjected to vertical tensile stress Σ^o (Figure 9). Horizontally, they are not subjected to any external stress. Their height is equal to three times their length L to avoid any disturbing boundary effect. We study four different values of a/L: 3/22, 4/22, 5/22, and 6/22, where a is the crack initial size. The effect of the quality of the discretization is characterized by the ratio L/d (11, 22, 44 and 88).

The ultimate tensile strength Σ^{max}, the loading limit of each sample, is evaluated and compared to theoretical results [1]. This comparison is shown in Figure 10 and indicates a convergent behavior of the discrete model towards the predictions of the fracture mechanics. The propagation of cracks in more complex conditions is presented in [7].

6 BRITTLE RUPTURE

Fracture mechanics is based on the assumption that materials present cracks (visible or not). If they are not (or cannot be) represented, the material strength grows indefinitely. Material strength is limited in reality due to intrinsic microcracks, small imperfections, etc., that can be hardly described in a fracture mechanics approach. Macroscopic rupture criteria are then adopted to characterize strength of a given material, without the description of its microstructure. These criteria (Rankine, Mohr-Coulomb, Von Mises, etc.) indicate where cracks may propagate in case of brittle rupture, but cannot provide other

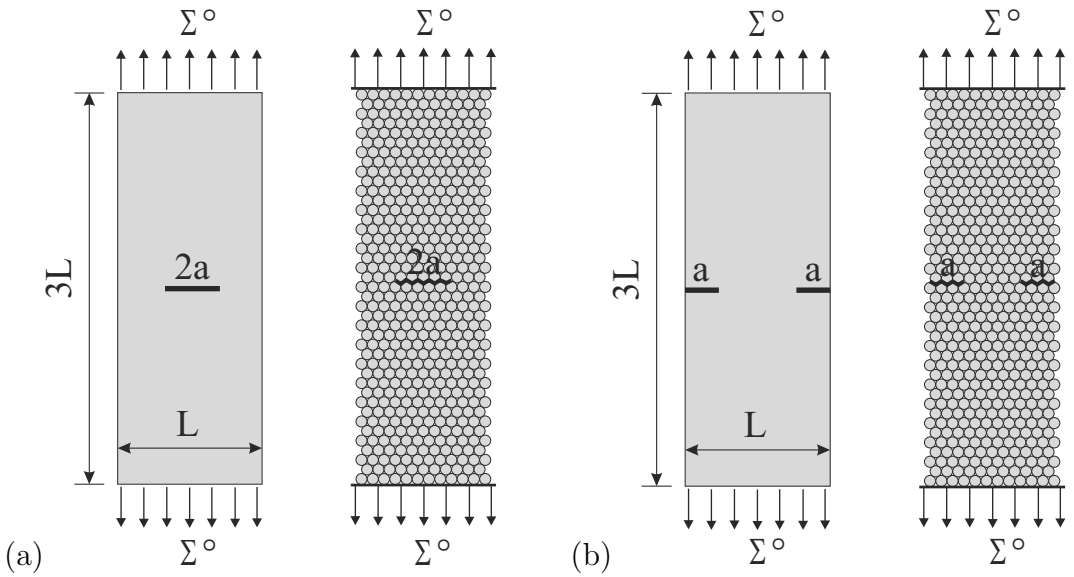

Figure 9: Tensile test on pre-cracked plates: (a) simple and (b) double cracks.

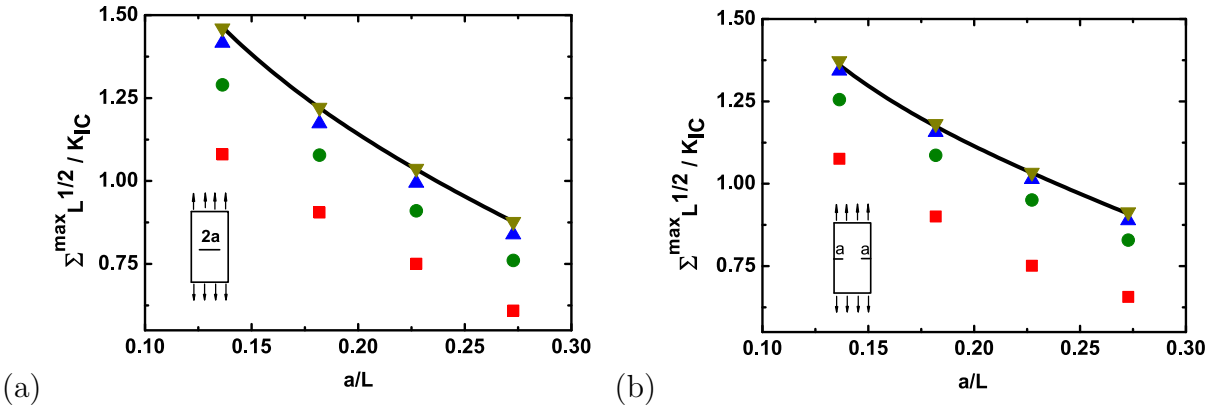

Figure 10: Maximal stress $\Sigma^{max}\sqrt{L}/K_{IC}$ as a function of initial crack lengths a/L for (a) simple and (b) double cracks. Discretization levels: (■) $L/d = 11$, (●) $L/d = 22$, (▲) $L/d = 44$, (▼) $L/d = 88$. The continuous lines correspond to the theoretical values [1].

important information like size and the number of cracks. This transition between macro and micro description of the material behavior, during the rupture, is well described by discrete approaches.

6.1 Tensile and compressive strengths

In absence of explicit cracks, we analyze the rupture of a sample submitted to bi-axial stresses (Figure 11a). From Equation 11, we can predict the tensile strength Σ^t, related to the material toughness:

$$\Sigma^t = K_{IC}\sqrt{2/(\pi d)}. \tag{12}$$

Tensile cracks are then expected to propagate orthogonally to the direction of the principal tensile stress $\overline{\sigma}_{\theta\theta}(\theta_0)$. However, compression cracks are parallel to the direction of the principal compression stress. To treat this issue, we define the maximum radial stress $\overline{\sigma}_{rr}(\theta_0)$ as (see Figure 7a):

$$\begin{aligned} \overline{\sigma}_{rr}(\theta_0) &= \overline{\sigma}_{II},\ if\ \beta \leq \pi/4, \\ \overline{\sigma}_{rr}(\theta_0) &= \overline{\sigma}_{I},\ if\ \beta > \pi/4. \end{aligned} \tag{13}$$

Similarly to $K_{\theta\theta}(\theta_0)$ (Equation 11), the stress intensity factor $K_{rr}(\theta_0)$ is defined as

$$K_{rr}(\theta_0) = \overline{\sigma}_{rr}(\theta_0)\sqrt{\frac{\pi d}{2}}. \tag{14}$$

Compression stress induce a negative value of the stress intensity factor $K_{rr}(\theta_0)$. This apparent inconsistency allows us to dissociate the effects of tensile and compression stresses, at the contact level. The choice of an inferior limit K^* for the negative values of $K_{\theta\theta}(\theta_0)$ implies for the compressive strength Σ^c:

$$\Sigma^c = K^*\sqrt{2/(\pi d)}, \tag{15}$$

where is K^* is completely independent of the material toughness K_{IC}.

6.2 Rupture envelope

We establish a rupture envelope based on bi-axial tests. Figure 11b shows the results for a material where $K^* = -10K_{IC}$ ($\Sigma^c = -10\Sigma^t$) for different discretization levels L/d: 44, 88 et 176, where L is the length of the square samples. Boundary effects are reduced for higher values of L/d explaining the convergence of the vertical and horizontal limit stresses (Σ_{yy}^{max} and Σ_{xx}^{max}, respectively) towards the theoretical (tensile and compressive) strengths. The observed behavior corresponds to the Rankine criterion, simply dependant on the values of principal stresses.

7 CONCLUSIONS

We present in this study a discrete model to deal with brittle rupture entirely compatible to continuous approaches. Hence calibration procedures are not necessary to characterize the stiffness and the strength of the material.

The analysis of the forces and displacements of a pair of adjacent contacts allow us to determine the stress and the strain tensors. At a local level, these information is associated to values of stress intensity factors, which lead to the description of crack propagation when compared to the material toughness. At a material scale, the crack opening is clearly related to the failure criterion of Rankine, defined by tensile and compressive strengths.

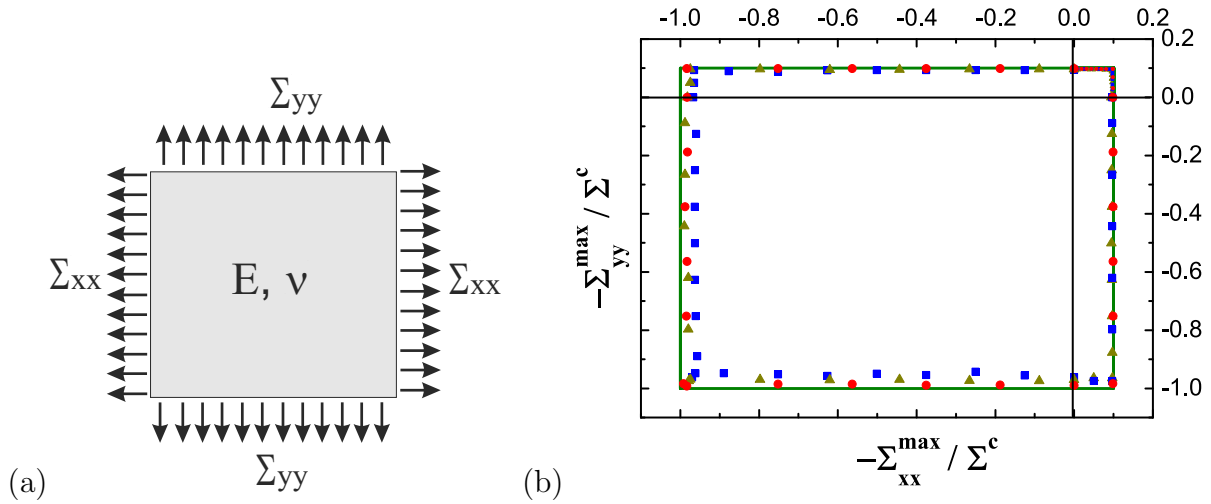

Figure 11: (a) Bi-axial load and (b) rupture envelope of the brittle material ($K^\star = -10K_{IC}$), for different discretization levels L/d : (■) $L/d = 44$, (▲) $L/d = 88$, (●) $L/d = 176$.

The definition of the contact rupture is physically consistent with the observations, considering the stress direction: tension induces orthogonal cracks, while compression induces parallel cracks.

The simulation results seems to converge monotonically to reference solutions depending on the discretization levels, described by the parameter L/d (number of particles adopted to represent a sample dimension). Globally, the observed convergence allows a systematic control of the reliability of the predictions of the model.

REFERENCES

[1] Bernard, B. *Notion pratiques de mécanique de la rupture*, Edition Eyrolles, (1980).

[2] Cundall, P. A. and Strack, O. D. L. A discrete numerical model for granular assemblies, *Gotechnique*, (1979), **29**, 1:47–65.

[3] Erdogan, F. and Sih, G. C. Crack extension in plates under plane loading and transverse shear, *J. Basic Eng.*, (1963) **85**:517–527.

[4] Koval, G. and Roux, J. N. and Corfdir, A. and Chevoir, F. Annular shear of cohesionless granular materials: From the inertial to quasistatic regime, *Physical Review E*, (2009), **79**, 1:021306.

[5] Labbens, R. *Introduction à la mécanique de la rupture*, Editions Pluralis, (1980).

[6] Le, B. D. and Koval, G. and Chazallon, C. Discrete element approach in brittle fracture mechanics, *Engineering Computations*, (2013) **30**, 2:263–276.

[7] Le, B. D. and Koval, G. and Chazallon, C. *Modélisation discrète en mécanique de la rupture des matériaux fragiles*, (2013), PhD thesis, INSA de Strasbourg, France.

[8] Tavarez, F. A. and Plesha, M. E. Discrete element method for modelling solid and particulate materials, *Int. J. Num. Meth. Engng.*, (2007) **70**, 379404.